

AISUENI, F., RAMALAN, M., ABUNUMAH, O., OGUNLUDE, P., ORAKWE, I., OGOUN, E., GIWA, A., SHEHU, H. and GOBINA, E. 2022. Gas diffusion, transport characteristics and modelling in porous membrane systems with application for polymer electrolyte membrane fuel cells. In *Proceedings of the 2nd International congress on scientific advances 2022 (ICONSAD'22), 21-24 December 2022, [virtual conference]*. Turkey: ICONSAD [online], pages 144-157. Available from: [https://en.iconsad.org/files/ugd/1dd905\\_c45aedd416d497e93113f00f465739b.pdf](https://en.iconsad.org/files/ugd/1dd905_c45aedd416d497e93113f00f465739b.pdf)

# Gas diffusion, transport characteristics and modelling in porous membrane systems with application for polymer electrolyte membrane fuel cells.

AISUENI, F., RAMALAN, M., ABUNUMAH, O., OGUNLUDE, P., ORAKWE, I., OGOUN, E., GIWA, A., SHEHU, H. and GOBINA, E.

2022

## Gas Diffusion, Transport Characteristics and Modelling in Porous Membrane Systems with Application for Polymer Electrolyte Membrane Fuel Cells

Florence Aisueni<sup>1</sup>, Muktar Ramalan<sup>1</sup>, Ofasa Abunumah<sup>1</sup>, Priscilla Ogunlode<sup>1</sup>, Ifeyinwa Orakwe<sup>1</sup>, Evans Ogun<sup>1</sup>, Ayo Giwa<sup>2</sup>, Habiba Shehu<sup>1</sup>, Edward Gobina<sup>1\*</sup>

e.gobina@rgu.ac.uk

<sup>1</sup> Centre of Excellence for Process Integration and Membrane Technology (CPIMT), School of Engineering, Robert Gordon University, Garthdee Road, ABERDEEN, AB10 7GJ, UK, Tel: +441224262348

<sup>2</sup> McAlpha, Inc., 205 - 279 Midpark Way SE, Calgary, ALBERTA T2X 1M2, CANADA,

**Abstract:** Fuel cells convert chemical energy in electrical energy and heat by consuming typically hydrogen and oxygen and producing water as the main by-product. This is achieved by reducing hydrogen at the anode (left hand side) and oxidising oxygen at the cathode (right hand side). The polymer electrolyte membrane fuel cell (PEMFC) gas diffusion layer (GDL) and the catalyst layer (CL) are crucial components mainly responsible for the distribution of gases, chemical reaction, and water transport in any PEMFC. The GDL consists of two main layers which are the macroporous substrate (MPS) and microporous layer (MPL). The MPS comes before the gas flow field and provides gas diffusion through a carbon-based paper or carbon cloth and collects the current. MPL is generally used to reduce the contact resistance between the CL and GDL. The most important parameters of porous membranes are derived from Fick's first law which relates the molar flux to membrane permeability. All possible gas transport mechanisms in porous membrane have been investigated in literature such as Hagen-Poiseuille, Knudsen, surface diffusion, capillary condensation, and molecular sieving.

**Keywords:** Polymer Electrolyte, Fuel Cells, Membrane, Gas Diffusion Layer, Catalyst Layer, Knudsen Number, Mean Free Path.

### INTRODUCTION

Figure 1 (left) describes the conventional electrode design for PEMFCs. In the PEMFC the gas diffusion layer (GDL) and the catalyst layer (CL) are crucial components mainly responsible for the distribution of reactant gases, chemical reaction, and water transport in. The GDL consists of two main layers which are the macroporous substrate (MPS) and microporous layer (MPL). The MPS comes before the gas flow field (Figure 1-right) and provides gas diffusion through a carbon-based paper or carbon cloth and collects the current. The membrane electrode assembly (MEA) is located between two graphite bipolar plates (GBPs), which collect electric current and enable gas feeding and cooling of the system. At the anode, H<sub>2</sub> is oxidized in the CL, releasing electrons, and generating protons. The electrons flow to the cathode through an external circuit, where they recombine with the protons in the CL and the oxidant (oxygen) to produce water. Proton transfer from the anode CL to the cathode CL through the polymer membrane thus closes the electrical circuit. The overall reaction differs from hydrogen combustion because a fraction of the Gibbs free energy can be converted into electric energy. MPL is generally used to reduce the contact resistance between the CL and GDL. In ultra-micropores the permeance is low but increase as pore sizes increase and depends on the Knudsen number,  $K_n$ . If the mean-free path of a molecule is less than 0.01 times the pore radius, ordinary diffusion is the primary mode of mass transport. If the mean-free path is greater than

ten times the pore radius, Knudsen diffusion dominates. This means that Knudsen diffusion should be considered if the pore size is less than about 0.5  $\mu\text{m}$ . The typical gas diffusion layer (GDL) of a PEMFC has pores between 0.5 and 20  $\mu\text{m}$  in radius, and a microporous layer contains pores between 0.05 and 2.  $\mu\text{m}$  in radius. Therefore, depending upon the material used, Knudsen diffusion may not have to be considered in GDLs, but it should be accounted for in microporous (MPL, MPS) and catalyst layers (CLs) respectively. When the mean free path of the gas molecules is comparable to the pore diameter, the flow mechanism is governed by the combined effect of both, the viscous and Knudsen mechanisms. Calculations based on Knudsen theory reveal that the gas transport in micropores is dominated by Knudsen diffusion, so most of gas kinetic energy was consumed on the collisions between the gas molecules and the pore wall, with only a small amount of gas arriving at the CL to take part in the oxygen reduction reaction (ORR). ORR is the most important cathodic process in PEMFCs. It should be noted that while micropores should be avoided in the GDLs, they are desired in the catalyst layers (CLs). Because the collisions between gas molecules and pore walls were desired as many as possible for the catalysts in the CLs to function more efficiently. This can help to explain experimental results achieved, but without explanation, in the recent study [1].

!

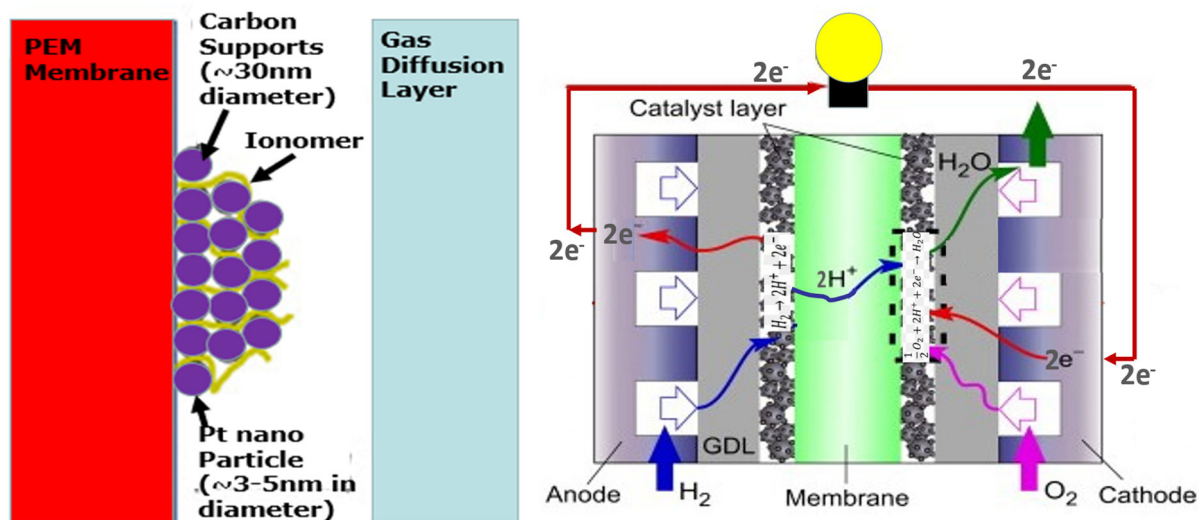


**Figure 1:** Conventional electrode design for PEM fuel cells (left) and schematic of PEM fuel cell showing details the inside workings (right)

## LITERATURE REVIEW

A membrane electrode assembly (MEA) is the heart of PEMFCs. In a MEA, CLs, and gas GDLs are considered as key components to deliver the protons generated on the surface of electrodes to polymer membrane and transfer of fuels in gaseous state to the electrodes. It also enhances the management of water generated from CL to the outlet in PEMFC system [2]. An effective catalyst structure consists of proton conductive ionomers and an electrode, forming three phase boundaries with fuel gases [3]. It therefore influences the intrinsic electrochemical properties of MEA such as catalyst activity, ohmic resistance and transport overpotential [4].

## EXPERIMENTAL

### Materials

Three kinds of commercial ceramic membranes have been used with pore size of 15 nm, 200 nm, and 6000 nm respectively. All the membranes are commercially available and were used as received without any further modifications. The ceramic membranes are tubular with an active separation length of 350 mm and 5mm glazed ends to enable incorporation of seals. To have a better understanding of the nano membranes, images of the membranes have been

analysed using scanning electronic microscopy with energy dispersive x-ray (SEM/EDAX) and contact angle.

## Methods

### Membrane Characterization

The functional groups in the membrane have been investigated using a Zeiss model Evo LS10 Scanning Electron Microscope (SEM) (Figure 2-left) with an Oxford Instruments INCA System Energy Dispersive X-Ray analyser (EDAX) (Figure 2-right) was used to determine the morphology and elemental composition of the prepared membrane. The Theta Flow is the premium contact angle meter (Figure 2-right) was used for static and dynamic contact angle measurements and surface energy measurements.

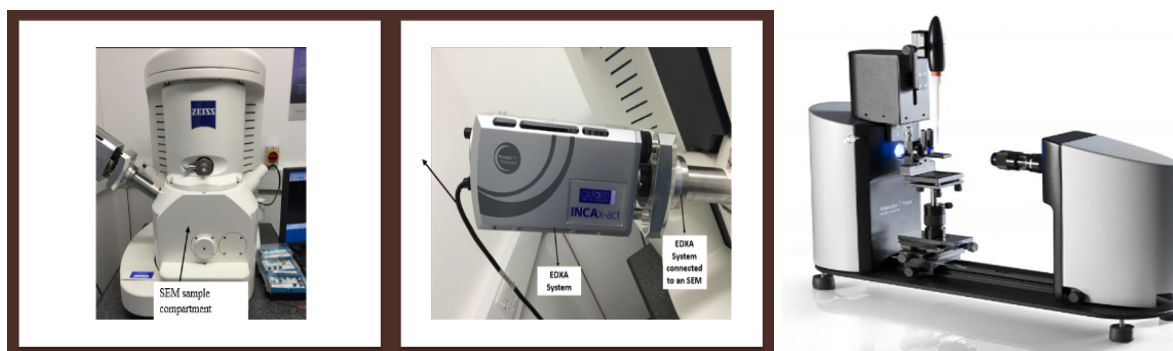


**Figure 2:** 1 Scanning Electron Microscope (SEM) (left) with an Oxford Instruments INCA System Energy Dispersive X-Ray analyser (EDAX) (middle) and Theta Optical Tensiometer (right)

### Gas Permeation Test

To evaluate the performance of the membrane, a reactor fitted with digital pressure gauges, control valves, piping and fittings, and Cole-Palmer digital flow meter has been used to determine the movement of the gases through the membrane. Gas permeation tests have been carried out with single-component gases, namely, carbon dioxide (99.5%), helium (99.5%) oxygen (99.5%) and nitrogen (99.5%) as supplied by BOC, United Kingdom. A schematic diagram of the gas transport system showing the x-section of the permeator cell and membrane is presented in Figure 4. The gas permeation experiment was performed by pressurising one end of the shell-side with the gas while keeping the other end at atmospheric pressure. The permeate end of the reactor was connected to flow meter to measure the flow of the permeated gas (L/min). The flow rate was converted to molar flow rate (mol/s) and normalised by dividing with the active membrane area to determine the flux of the gases through the membrane. Transmembrane pressure was controlled by a pressure controller and the flow of the gases through the membrane was measured with a digital flow meter. The system can be operated in a retentate flow-through mode or dead-end mode as detailed in GOBINA, US Granted Patent 7048778 [5].

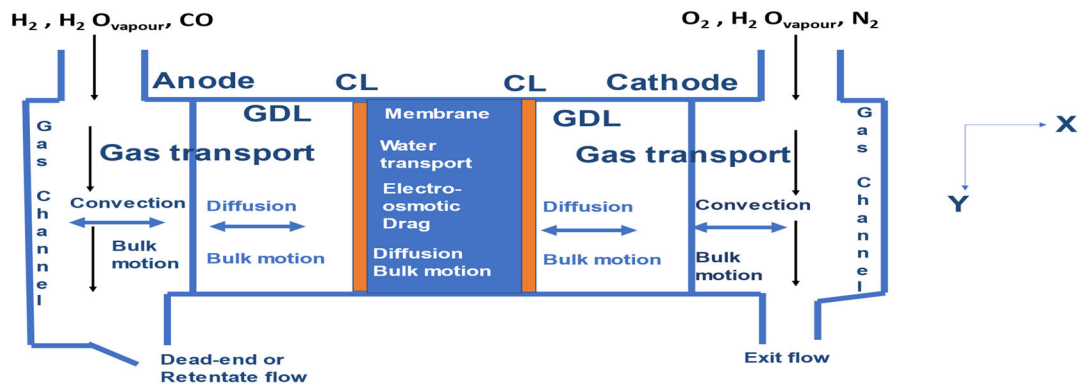
## MASS TRANSFER MODELLING IN PEMFC SYSTEMS

Figure 3 shows the schematic diagram of the inside of the PEMFC and the mass transfer phenomena. It is divided into gas diffusion layers (GDLs), catalyst layers (CLs), and an electrolyte membrane. It is composed of a fuel electrode in which hydrogen ion (proton) is produced, an electrolyte that allows the selective transport of proton, and an air electrode in which oxygen contained in the air feed react with incoming protons exiting the membrane and electrons coming via an external circuit to produce water. The modelled single fuel cell is represented schematically in Figure 3 shows the input reactant gases – hydrogen at the anode

and oxygen at the cathode, flow in channels in the y-direction. Both flows reach the catalyst layers (CL) by transport through the two GDLs (x-direction). There, reactants are consumed, and water is produced at the cathode side.

The water flowing in the membrane is absorbed on one side and desorbed on the other. The following transport phenomena occur. First, the motion of the gas molecules can be either by bulk transport, by convection, and/or by diffusion. Second, the gases fed in are not usually pure, but contain nitrogen (in the air), water (humidification) and trace concentrations of other gases (CO, nitrogen compounds etc.) whose effects must be considered. Third, the motion of the water molecules inside the membrane is also affected by the electro-osmotic drag, which corresponds to the water transport relating to the proton transport from the anode to the cathode, and which acts in addition to the usual convection and diffusion. And fourthly, from a practical point of view, the hydrogen supply can be either retentate flow-through or dead-end (the air supply is always retentate flow-through). Water transport in the cathode catalyst layer (CCL) of a PEM fuel cell involves several transport and physical processes: (a) electro-osmotic transport of water from the membrane to the CCL, (b) back-diffusion of water from the CCL to the membrane, (c) condensation and evaporation of water, and (d) removal of liquid water to the gas flow channel through the GDL. The electro-osmotic transport occurs due to the proton transport. Proton migrations drag water along with it from the anode side to the cathode side and that can eventually reduce the membrane hydration and block the active reaction site in the CCL. Conversely, the back-diffusion represents the water transport back to the membrane due to the concentration gradient. Since water is produced at the CCL and protons are dragging liquid water from the anode side, the liquid water concentration in the cathode side increases significantly compared to the anode side during the operation of fuel cells. This concentration difference causes diffusion of water from the CCL to the membrane.

Further, if the reactant gases are fully humidified, water vapours in the gas mixture tend to condense. Conversely, if the gases are partially hydrated, liquid water will start to saturate the gas mixture through the evaporation process. Furthermore, the liquid water can be removed from the cathode GDL by the flow of reactant gas in the gas flow channel that can eventually dry out the electrode, hence the membrane, if the rate of water removal is too fast. Clearly, the entire water transport process in a PEM fuel cell is a complex phenomenon, hence it is essential to make a delicate water balance (engineered CL ionomer) for better and optimum fuel cell performance and prevent material degradation due to flooding.



**Figure 3:** Schematic of mass transfer phenomena in PEM fuel cells showing the gas diffusion layer (GDL)

### Free Molecule (Knudsen) Flow in Porous Media

Knudsen or free-molecule flow occurs when gas molecules collide more with the walls of the container than with each other. Knudsen flow occurs when the mean free path of the gas molecules is approximately the length scale of the container, or there are very low gas densities, (which means large mean free paths). In free molecule flow, there is no distinction between flow and diffusion (which are molecular phenomena). Also, gas composition is not important since there is no interaction between gas molecules of the same or different species.

$$F_{kn,0} = \frac{2 \cdot \epsilon_p \cdot \mu_{Kn} \cdot \bar{v} \cdot \check{r}}{3RTL} \text{ with } \bar{v} = \sqrt{\frac{8RT}{\pi M}} \quad (1)$$

Where  $F_{Kn,0}$  is the Knudsen permeation ( $\text{mol} \cdot \text{m}^{-2} \cdot \text{s}^{-1} \cdot \text{Pa}^{-1}$ ),  $\epsilon_p$  is the porosity (—),  $\mu_{Kn}$  is a shape factor (—) equal to  $1/\tau$ , where  $\tau$  is the tortuosity,  $R$  is the gas constant ( $\text{J} \cdot \text{mol}^{-1} \cdot \text{K}^{-1}$ ),  $T$  is the absolute temperature (K),  $\check{r}$  is the modal pore radius (m),  $\bar{v}$  is the average molecular velocity ( $\text{m} \cdot \text{s}^{-1}$ ),  $L$  is the layer thickness (m) and  $M$  is the molecular mass ( $\text{kg} \cdot \text{mol}^{-1}$ ) of a gas molecule.

### Ordinary (Molecular) Diffusion in Porous Media

Ordinary diffusion is the most common diffusion mechanism. For binary mixtures, the diffusive flux is directly proportional to its concentration gradient. In multicomponent mixtures, the fluxes of all the species should be considered since it affects the diffusive transport of any one species. This is because the momentum transferred to any one species will depend on the relative motion of all other species. The flux of a single species can be calculated in terms of the concentration gradients of the other species using Fick's law of diffusion:

In the general case, at a constant temperature and pressure, the molar diffusion flux  $\dot{n}$  ( $\text{mol} \cdot \text{m}^{-2} \cdot \text{s}^{-1}$ ) of substance A is directly proportional to  $dC_A/dy$  known as the molar concentration gradient ( $\text{mol}/\text{m}^3\text{m}$ ) and a one-dimensional formulation is described by Fick's law. (Equation (6)).

$$\dot{n}_A = -D_A \frac{dC_A}{dy} \quad (2)$$

Where  $D_A$  is the diffusion coefficient (m/s) in a binary system. The flow of one component must be balanced by the counterflow of the other component and therefore

$$\dot{n}_B = -D_B \frac{dC_B}{dy} \quad (3)$$

but since  $C_A + C_B = \text{constant}$ , then

$$\left| \frac{dC_A}{dy} \right| = \left| \frac{dC_B}{dy} \right| \text{ and } D_A = D_B = D_{AB} \quad (4)$$

$D_{AB}$  is known as the interdiffusion coefficient. In order to describe a unidirectional diffusion of molecules A in a multicomponent mixture of ideal gases, the Stefan-Maxwell equation (5) is used

$$\frac{dY_A}{dy} = \sum_{j=A}^n \frac{d_A C_j}{C_A^2 D_{Aj}} (\mathbf{u}_j - \mathbf{u}_A) \quad (5)$$

Equation (9) is based on the kinetic theory of gases, in which  $Y_A$  is the mole fraction of component A;  $C_T$  is the total concentration (density) of mixture ( $= p/RT$ );  $C_A = pY_A/RT$ ;  $c_j = pY_j/RT$ ;  $D_{Aj}$  is the interdiffusion coefficient for a pair A, j; and  $u_j$  and  $u_A$  are the rates of diffusion for the components of the pair respectively.

#### Viscous (Darcy) Flow in Porous Media

Viscous (Darcy) flow refers to flow in the laminar continuum regimen that is caused by a pressure gradient. The gas behaviour is determined by the coefficient of viscosity, which is independent of pressure for gases. Since bulk flow does not separate the components of gas mixtures -- mixtures of different gasses can be treated in the same manner as a pure gas. Under laminar flow conditions, the single-phase flow of incompressible fluids in porous media is governed by Darcy's law described by Equation 6.

$$F_{P,0} = \frac{\epsilon_p \mu_p}{8RT} \frac{\bar{r}^2}{\eta L} P_m \quad (6)$$

Where  $F_{P,0}$  is Poiseuille permeation ( $\text{mol.m}^{-2} \cdot \text{s}^{-1} \cdot \text{Pa}^{-1}$ ),  $\mu_p$  is the reciprocal tortuosity ( $-$ ),  $\eta$  is the gas viscosity ( $\text{N.s.m}^{-2}$ ),  $L$  is the thickness of the porous layer (m) and  $P_m$  is the mean pressure (Pa). Laminar flow is also sometimes referred to as viscous or streamline flow. Typically, this type of flow occurs at lower velocities, and the fluid flow is characterised by the absence of lateral mixing. At low Reynolds number when the viscous forces dominate, they are sufficient to maintain all the fluid particles in line, and then the flow is laminar.

#### PEMFC KEY COMPONENTS

The PEMFC consists of a gas diffusion layer and an electrode on each side, and a polymer electrolyte membrane in between the electrodes. The electrode-membrane assembly is usually constructed in between the pressurized hot plates.

#### Separators

The separators are located so that they sandwich the cell. They are made up of electrically conductive carbon or similar plates. Fine grooves are cut in their surfaces to allow hydrogen or air to pass and be supplied to the electrodes.

#### Cell Stack

A cell stack is composed of single cells stacked on one another. Connecting them in series allows a high voltage and large power to be extracted.

#### Gas Diffusion Layer (GDL)

There over 20 different commercially types of GDLs The GDL in can consist of a single layer or a double layer (GDL and a MPS). The GDL causes the gases to spread out to enable maximum contact surface area with the CL. The thicknesses of various gas diffusion materials can vary between 0.0017 and 0.04 cm with a porosity ranging between 70% and 80%. The most used GDL materials are carbon cloth and carbon. The GDL must retain good conduction, be chemically stable and able to withstand the operating temperatures and compression loads of the fuel cell stack. Several methods that have been used to model the GDL and some of the more conventional methods include modelling the gas and fluid transport through the pores or modelling the interaction of the gas or water with the solid porous media. Commonly used

modelling methods include Fick's Law, Darcy's Law, and the Stefan-Maxwell diffusion equations for the mass transport.

### Catalyst Layer (CL)

CLs are the critical components within fuel cells as they are the location where the electrochemical reaction occurs. The structure and morphology of the CLs are important to minimize electrochemical resistance and thus obtain high single cell efficiency. CLs can be fabricated by various coating methods such as screen printing and spraying and can be characterized by the SEM/EDAX images of the surface, pore distributions using BET, and electrochemical performances. Ionomers are ion containing polymers used to deposit the catalyst.

### Membrane

Perfluorinated sulfonic acid ionomers (Nafion) are most often used as ion-selective membranes. Important applications include cation exchange membrane for fuel cells and PEM water electrolyzers.

### Anode

Figure 4 (left) shows an enlarged schematic cross-section of the anode GDL constituted by a macro-porous substrate MPS and a MPL, CL and PEM. Pressure is another important parameter for performance improvement in a PEMFC. However, compared to the cathode, the pressure drop in the anode can safely be neglected since it is much less significant.

### Cathode

Figure 4 (right) shows a schematic of the cathode side of the membrane–electrode assembly showing an enlarged schematic cross-section of the cathode gas diffusion layer constituted by a MPS and a MPL, CL and PEM. Oxygen or air flows through the gas flow channel and must diffuse through the GDL to the CL where it reacts with protons coming through the polymer PEM to make water. The water formed must leave the CL layer and go through the GDL into the gas flow channel where it can be carried out of the fuel cell. Some water may also enter the polymer electrolyte membrane. During high current density operation, the high-water production in the PEMFC cathode CL can negatively affect performance by lowering mass transport of oxygen into the cathode. In this paper, a novel heat treatment process for controlling the ionic polymer/gas interface property of the fuel cell catalyst layer is investigated and then incorporated into the membrane electrode assembly (MEA) fabrication process.

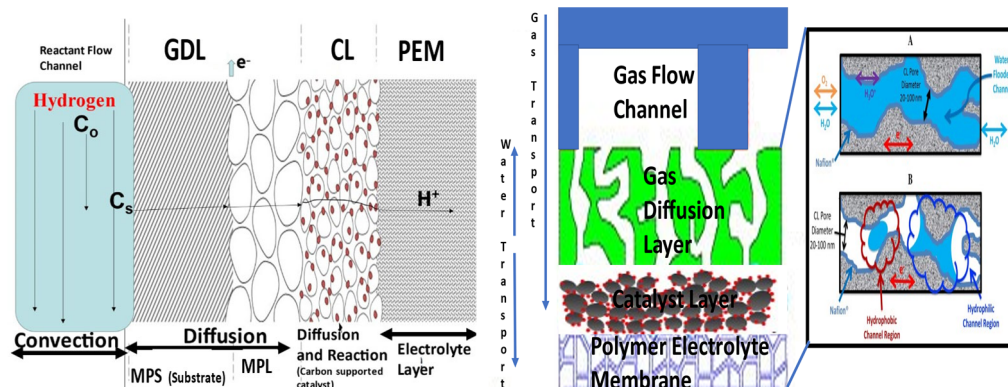


**Figure 4:** Mass transfer schematic cross-section of the anode side of the MEA (left) and cathode (right) of a typical PEMFC showing a cross-sectional side view of (A) water-flooded CL pore and (B) engineered CL ionomer surface on the cathode side. §

§

## RESULTS

Figure 5 shows the real photograph of the experimental setup from left to right. The whole setup includes a stainless-steel shell and tube permeator with the membrane tube centralised using two “o” ring seals at both ends to create shell-side inlet and exit and tube-side inlet and exit. By closing or opening valves located at these inlets and exits the feed gas can be directed to permeate the porous membrane and the flowrate monitored and measured at the exit. Table 1 gives an overview of the applied single gas permeation test conditions. Single gas permeation tests of H<sub>2</sub>, He, air and O<sub>2</sub> were carried out for the 15nm, 200nm and 6000nm samples at 373 K and feed pressures drops of 0.2 – 3.0 bar with the permeate side kept at atmospheric pressure. No sweep gas was used in the permeation test and the retentate side was closed

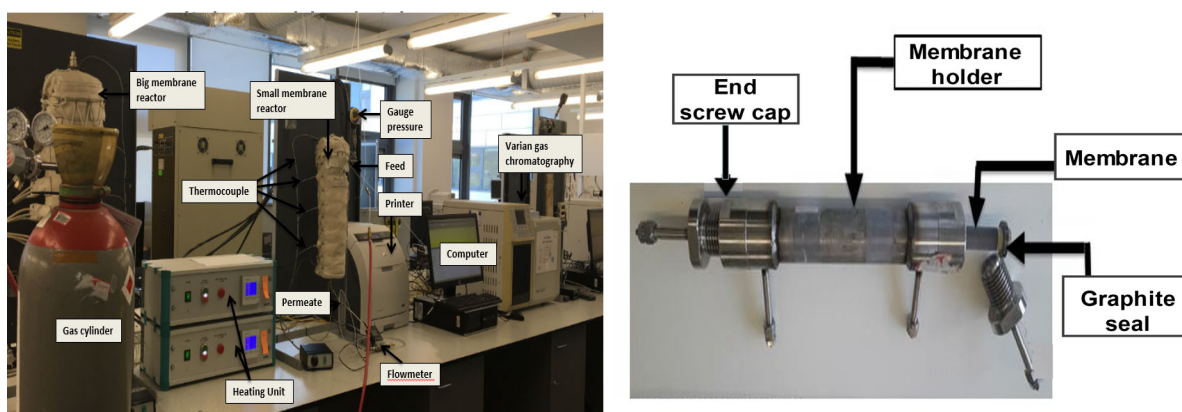


**Figure 5:** Pictorial representation of the flow system used in the permeation experiments (left) and Real picture of the stainless-steel shell and tube permeator with the membrane tube showing the “O” ring seal (two were used one at each end), the membrane and end screw caps.

**TABLE 1:** RELEVANT PROPERTIES AND TEST CONDITIONS OF GASES USED FOR THE PERMEATION TESTS AND THEIR CRITICAL TEMPERATURES AND PRESSURES

Gas	Kinetic diameter, 10 <sup>-12</sup> m	Molecular mass, g/mol	Critical temperature, K	Critical pressure, bar	Tested pressure range, bar	Pressure drops, bar	Tested temperature, °C
He	260	4	13.0	2.24	1.2-4.0	0.2-3.0	20 and 100
H <sub>2</sub>	289	2	33.3	12.97	1.2-4.0	0.2-3.0	20 and 100
O <sub>2</sub>	346	32	154.6	50.5	1.2-4.0	0.2-3.0	20 and 100
Air	371	29	52.2	549.08	1.2-4.0	0.2-3.0	20 and 100

## Membranes

All the membranes used are commercially available. The 15 nm pore size tubular membranes consist of 77% Al<sub>2</sub>O<sub>3</sub> and 23% TiO<sub>2</sub> with the porosity of 45%. The 6,000 nm was an  $\alpha$ -alumina membrane with a TiO<sub>2</sub> washcoat while the 200 nm was a mesoporous  $\gamma$ -alumina/ $\alpha$ -alumina composite membrane. All membranes were supplied by Ceramiques Techniques et Industrielles (CTI SA), France and were used as received without any further modifications. The permeators were sized to handle membranes with 10 mm outside diameter or 25 mm outside diameter. Real pictures of the membranes used are show in Figures 6, 7 and 8 respectively



Figure 6: Picture of 15nm (25mm OD) membrane



Figure 7: Picture of 200nm (10mm OD) membrane



Figure 8: Picture of 6,000nm (25mm OD) membrane

#### SEM/EDAX

SEM shows large pores are observed for the 6000 nm membrane although the 6000 nm membrane particles are more densely packed presenting a low porosity. The elemental analysis by EDAX indicates that the membranes contain Al and O, whereas the presence of the little amount of Ti, Si, C, P and S appear because of the acidic inclusions from the other solutions used in layers added to systematically reduce the pore size to 15 nm.

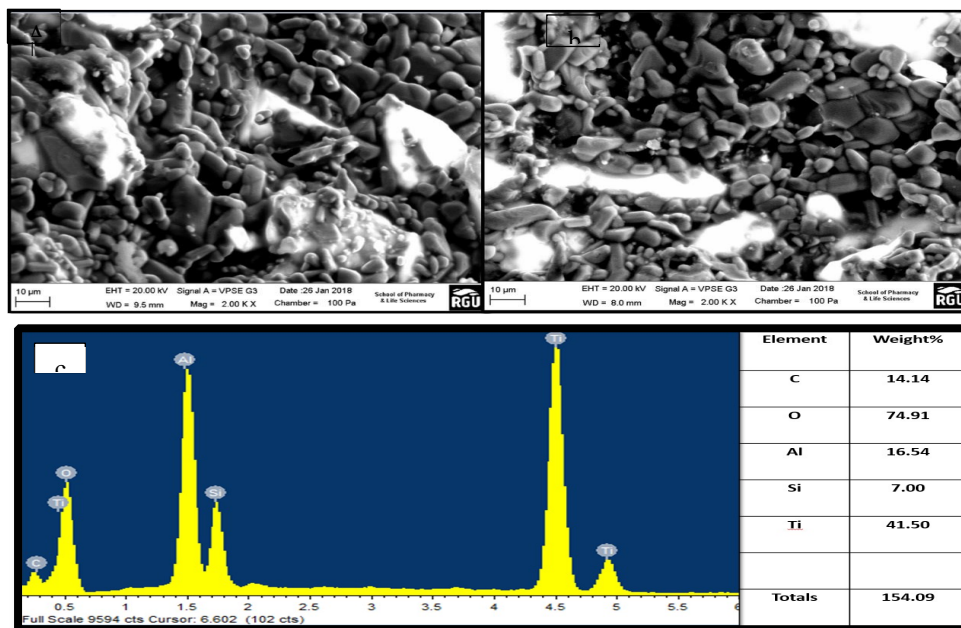
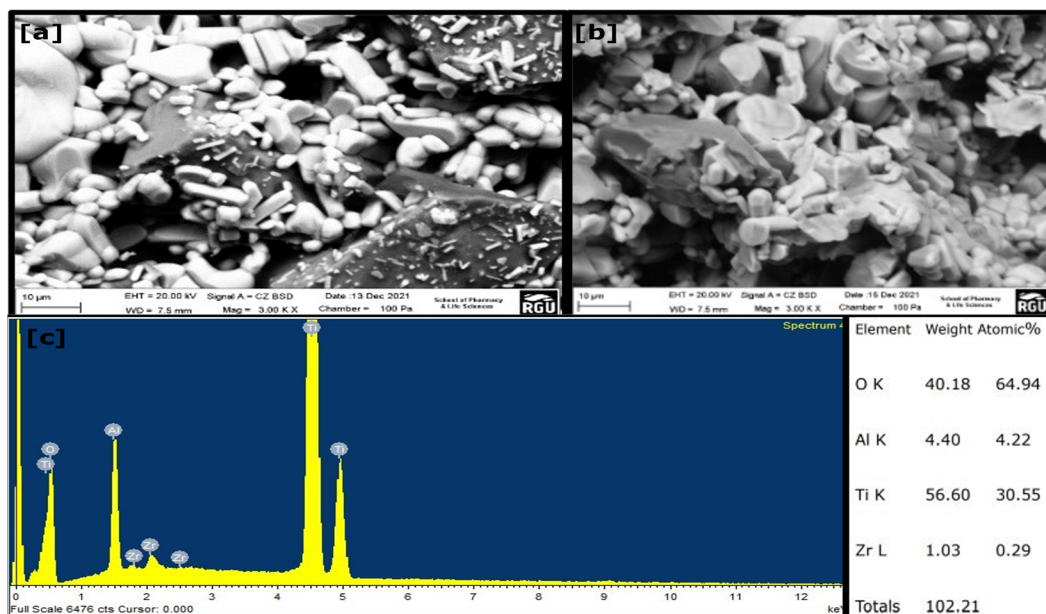
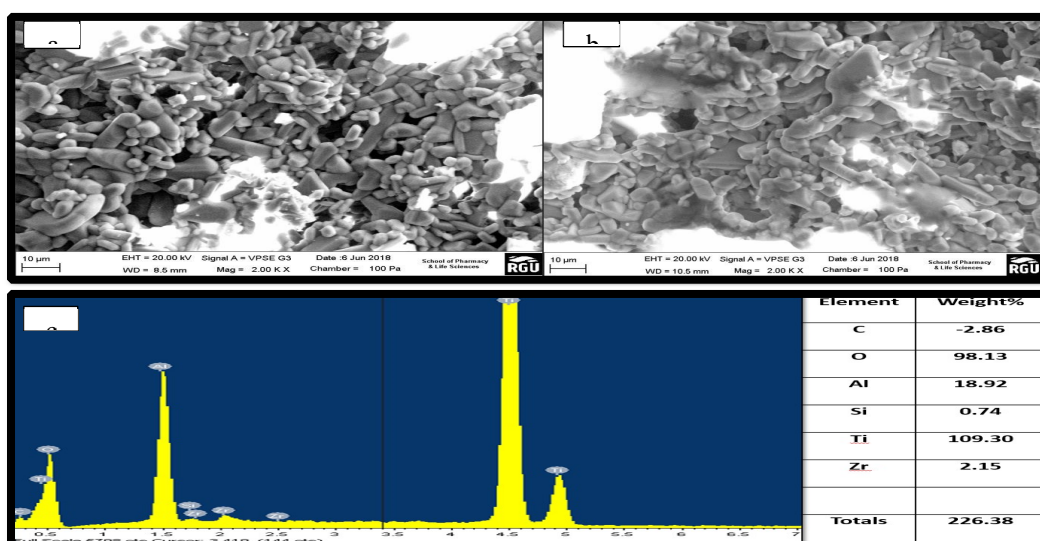


Figure 9: Micrographs for 6000 nm  $\alpha$ -Al<sub>2</sub>O<sub>3</sub> support: (a) inner surface, (b) outer surface and (c) EDAX showing the chemical compositions of the outer surface.



**Figure 10:** Micrographs for 200 nm  $\alpha$ -Al<sub>2</sub>O<sub>3</sub> support: (a) outside surface, (b) x-section and (c) EDAX showing the chemical compositions of the outer surface.



**Figure 11:** Micrographs for 15 nm  $\alpha$ -Al<sub>2</sub>O<sub>3</sub> support: (a) inner surface, (b) outer surface and (c) EDAX showing the chemical compositions of the outer surface.

Effect of the pore size on contact angle, surface tension, capillary pressure, and surface free energy, for the three different membranes

Figure 12 shows the contact angle measurements for 15nm (left), 200nm (middle) and 6,000nm (right) membranes. In a hydrophilic catalyst layer ( $\theta_c < 90^\circ$ ), the CCL having a contact angle of  $89^\circ$  shows significantly higher liquid saturation than the CCL having lower contact angle or higher wettability. It is mainly due to the capillary pressure.

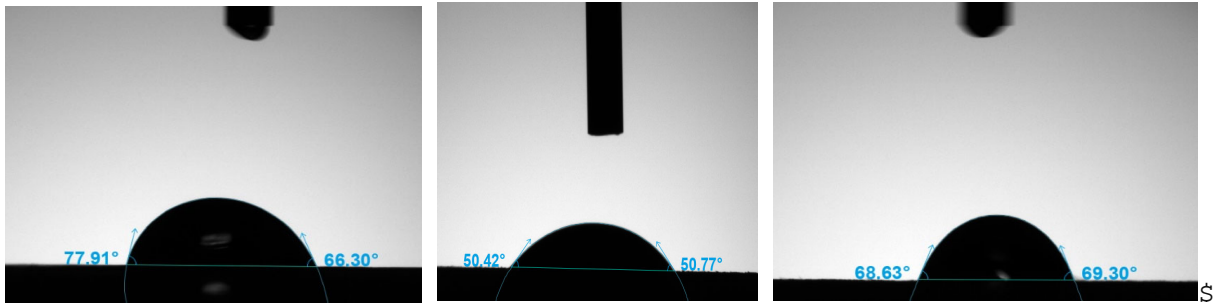


**Figure12:** Contact angle measurements for 15nm (left), 200nm (middle) and 6,000nm (right) membranes.

Table 2 shows that the 200nm pore membrane has the lowest contact angle but highest surface free energy. The surface free energy is the work required to form the surface, while surface stress indicates the work required to extend the surface. In the case of a two-fluid interface, there is no demarcation between forming and stretching because the fluids and the surface completely replenish their nature when the surface is extended. Therefore, the force that attracts the molecules to each other on the surface of a liquid is called the surface tension and is referred to as surface energy in solids.

**TABLE 2:** EXPERIMENTAL RESULTS FOR CONTACT ANGLE OF THE DIFFERENT NANO MEMBRANES

Ceramic Membrane Pore Size (nm)	Contact Angle [θ]	Surface Free Energy $y^{tot}$ [mN/m] / $y^d$ [mN/m]
6000	63.687	43.14 / 43.14
200	36.924	59.625 / 59.625
15	76.642	37.58 / 37.58

## DISCUSSION

### *Knudsen number and mean free path*

As gas molecules travel through the pores of GDL, CL, MPL and MPS, one of three mechanisms can occur, and depending on the specific nature of the diffusing gas constituent and the intrinsic microstructure of the layer. The three mechanisms of molecular diffusion, viscous diffusion, and Knudsen diffusion could happen. To distinguish among these three mechanisms, the Knudsen number ( $K_n$ ) is typically invoked, as shown in Equation 7 [6].

$$K_n = k_B T / [2^{0.5} P (22/7) (d_g)^2 d_p] \quad (7)$$

Where:

$d_p$  = diameter of the pores (m)

$P$  = gas pressure (atm)

$d_g$  = effective diameter of a gas molecule (m)

$k_B$  = Boltzmann constant ( $1.3807 \times 10^{-23}$  J K<sup>-1</sup>)

$T$  = temperature of the gas (K)

The Knudsen number is the ratio of mean free path of gas molecules to the system length scale as given by Equation 8.

$$Kn = \lambda / d_p. \quad (8)$$

In Equation 8,  $\lambda$  is the mean free path (m) and is defined as the distance traversed by a gas molecule from one collision to the next and  $d_p$  is the pore diameter (m). The pore sizes in GDLs and MPLs are within 1–150  $\mu\text{m}$ , and 2–200 nm, respectively. Figure 13 shows how the Knudsen number varies with transmembrane pressure drop for each membrane at 100 °C for feed gases to the PEMFC. He is used as a control.

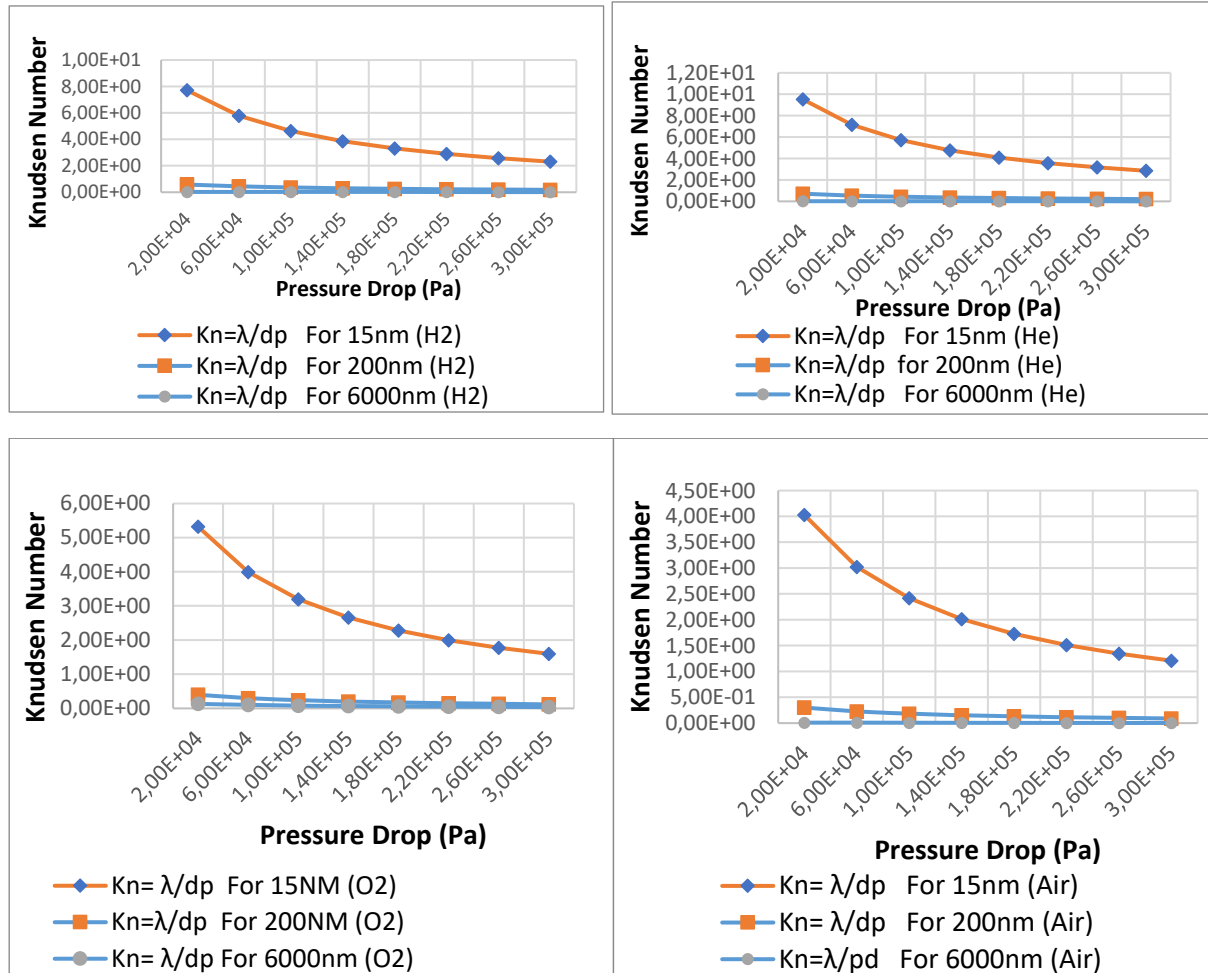


**Figure 13.** Effect of transmembrane pressure drop on Knudsen number at 100 °C for He (top left), H<sub>2</sub> (top right), O<sub>2</sub> (bottom left) and Air (bottom right)

### Pore structure

Pore structure is crucial for the application of PEMFC materials for construction of GDLs, CLs, MPS and PEM. In general, the pores of these materials are formed by different methods. The common technique adopted in this study for pore characterization is the BET (gas absorption). BET method combined with Barrett-Joyner-Halenda (BJH) analysis to determine pore size distribution. BET method is suitable to characterize micro- or mesoporosity below the effective range of mercury intrusion porosimetry. The main feature of complete wetting is the absence of contact angle hysteresis. During the first stage the contact angle decreases, and the spreading area increases, until the maximum value of the spreading area is reached. The Knudsen number obtained was between 4-10 and enabled the correspondence between GDL pore scale and Knudsen-number-based gas diffusion mode as shown in Figure 14 (left). The calculation based on Knudsen theory revealed that the gas transport in micropores is dominated by Knudsen diffusion so most of gas kinetic energy is devoured on the collisions between the gas molecules and the pore wall, with only a diminutive amount of gas arriving at the CLs to

take part in the oxygen reduction reaction (ORR). It should be noted that while micropores should be avoided in the GDLs, they are desirable in the CLs. Because the collisions between gas molecules and pore walls are preferable micropores are needed for the catalysts in the CLs to high conversion rates of feed stock.

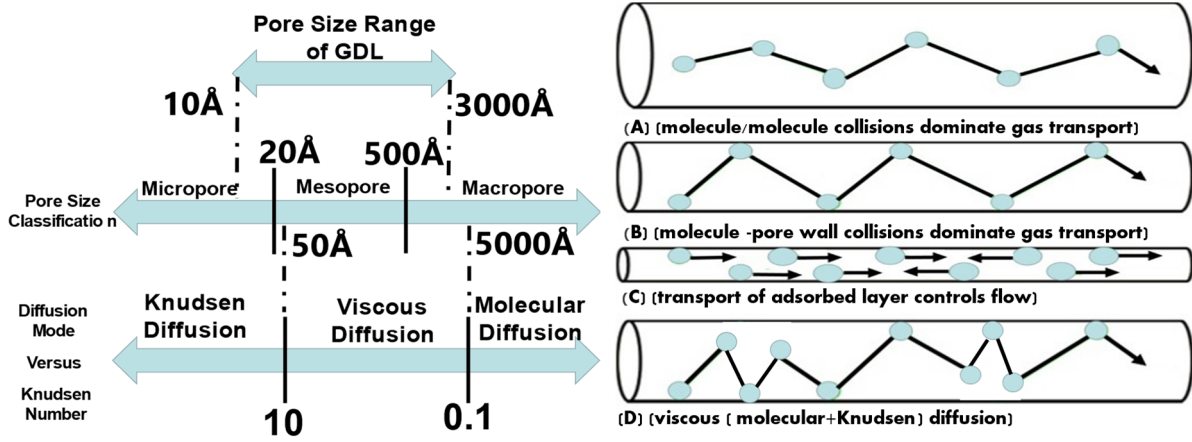


**Figure 14:** Schematic diagram of the correspondence between GDL pore scale and Knudsen-number-based gas diffusion mode (left) and basic macroporous substrate and microporous gas transport mechanisms in porous media (A = Pure molecular diffusion, B = Pure Knudsen diffusion, C = Adsorption and D = Viscous (Molecular + Knudsen) diffusion) (right)

From our model equations (1-6) above, permeation through the support can be expressed to take account for both viscous and Knudsen flow. When the number of intermolecular collisions is strongly predominant ( $K_n \ll 1$ ), the flow mechanism is governed by viscous flow (recall Equation 6).

$$F_{p,0} = \frac{\epsilon_p \mu_p}{8RT} \frac{\bar{r}^2}{\eta L} P_m \quad (6)$$

Knudsen diffusion occurs when the number of molecules-wall collisions is dominant ( $K_n \gg 1$ ). Knudsen flux is dependent on the molecular weight of the diffusing species. With this mechanism, light molecules go through the pores faster than heavy molecules under the same concentration gradient (recall Equation 1)

$$F_{kn,0} = \frac{2\epsilon_p \mu_{Kn} \bar{v}}{3RTL} \text{ with } \bar{v} = \sqrt{\frac{8RT}{\pi M}} \quad (7)$$

When the mean free path of the gas molecules is comparable to the pore diameter, the flow mechanism is governed by the combined effect of both, i.e., the viscous and Knudsen mechanisms. For single gases the total flux through porous membrane layers the sum of Equation 1 and Equation 6 can be written as Equation 8.

$$F_{p,0} + F_{Kn,0} = \alpha_s + \beta_s P_{av} \quad (8)$$

Where:

- $\alpha_s$  = Knudsen flow contribution
- $\beta_s P_{av}$  = viscous flow contribution
- $P_{av}$  = average pressure (atm)

## Abbreviations and Acronyms

TABLE 3. UNITS FOR MEMBRANE DIMENSIONS

Sy m	Quantity	Conversion from Gaussian and CGS EMU to SI <sup>a</sup>
Å		10 <sup>-10</sup> m
k <sub>B</sub>	Boltzmann constant	1.3807 × 10 <sup>-23</sup> J K <sup>-1</sup>
nm		10 <sup>-9</sup> m
µm		10 <sup>-9</sup> m
R	Universal gas constant	8.31 J/mol K

## CONCLUSION

Mass transport in the fuel cell GDL, MPL, MPS and CLs are dominated by diffusion due to the tiny pore sizes of these layers (2 to 10 microns). In a flow channel, the velocity of the reactants is usually slower near the walls; therefore, this aids the flow change from convective to diffusive. This study demonstrates that porous membranes with precise pore sizes can be used to study PEM fuel cell structure of CL, GDL, MPL, MPS and CLs and was clear that different membrane structures with different morphology and various pore sizes can be adopted to reveal important characteristics of key PEM fuel cell components that can be used to improve performance.

## ACKNOWLEDGEMENT

This work is financially supported by matched funding from the Net Zero Technology Centre (NZTC), Scotland, UK and McAlpha, Inc., Calgary, CANADA.

## REFERENCES

- [1] X. Shi and T. Huang, "Effect of pore-size distribution in cathodic gas diffusion layers on the electricity generation of microbial fuel cells (MFCs)" RSC Adv, vol 5, pp. 102555-102559. 2015, DOI: 19.1039/C5RA19811A.
- [2] G. Shao, Z. Yin, Wang, Gao Y. "Proton exchange membrane fuel cell from low temperature to high temperature: material challenges" J Power Sources, 167, pp. 235-242, 2007.
- [3] H. Kuroki, T. Yamaguchi "Nanoscale morphological control of anode electrodes by Grafting of Methylsulfonic acid groups onto Platinum–Ruthenium-supported carbon Blacks, J Electrochem Soc, 153, pp. A1417-A1423, 2006
- [4] K.-H. Kim, K.-Y. Lee, H.-J. Kim, E. Cho, S.-Y. Lee, T.-H. Lim, *et al.* "The effects of Nafion® ionomer content in PEMFC MEAs prepared by a catalyst-coated membrane (CCM) spraying method" Int J Hydrogen Energy, 35 pp.2119-2126, 2010.
- [5] E. Gobina "A membrane apparatus and method for separating gases" US Granted Patent 7048778, 23-May-2006, <https://patents.justia.com/inventor/edward-gobina>
- [6] K. Keizer "Gas separation mechanisms in microporous modified  $\gamma$ -Al<sub>2</sub>O<sub>3</sub> membranes" Journal of Membrane Science, 39, pp. 285-300, 1988.